Chuka University
info@chuka.ac.ke | 020 231 0512 / 020 231 0518

ELECTRONIC PROPERTIES AND MAGNETIC ORDER OF COMPOSITIONALLY AND STRUCTURALLY RE-ARRANGED HEUSLER COMPOUND Mn_2CoAl

Muthui, Zipporah Wanjiku
Department of Physical sciences, Chuka University, P. O. Box 109-60400, Chuka, Kenya Email: ciku32ke@yahoo.com or zwanjiku@chuka.ac.ke

How to cite:
Muthui, Z. W. (2021). Electronic properties and magnetic order of compositionally and structurally re-arranged heusler compound Mn2CoAl. *In: Isutsa, D. K. (Ed.). Proceedings of the 7th International Research Conference held in Chuka University from 3rd to 4th December 2020, Chuka, Kenya, p. 598-604*

ABSTRACT
Heusler compound Mn_2CoAl has been reported to possess the spin gapless property. It has been proposed as a candidate for application in fabrication of spin-logic and energy efficient spintronic devices. While some theoretical studies have reported a ferromagnetic order in the ordered alloy, some have reported a ferrimagnetic order. Some reports have found the regular $L2_1$ crystal structure more stable, while others have reported the inverse Heusler structure as being more stable. Recently, its ferrimagnetic order was observed experimentally using the synchrotron-based x-ray magnetic circular dichroism technique. These results have been explained using theoretical investigations of the interaction between the atom resolved states and magnetic moments using the Density Functional Theory (DFT), as implemented in the Quantum ESPRESSO package, for the compositionally ordered and disordered systems as well as distorted and un-distorted crystal structures. The exchange-correlation potential is treated with the Generalized Gradient Approximation (GGA), employing the Perdew-Burke-Ernzerhof (PBE) exchange-correlation functional (PBE-GGA). The inverse Heusler structure is found to be more stable than the $L2_1$ structure. There is a near zero gap in the majority states, while a clear gap at the Fermi level is evident in the minority states. Tetragonalizing the structure causes an increased intersection of the Mn *d* states at the Fermi level, causing the electronic structure to tend towards a half metal rather than a spin gapless semiconductor. Higher structural distortions destroy the half metallic gap, resulting in a metallic electronic structure. Intermixing of the states results in a half metallic electronic structure. The Mn magnetic moments couple antiferromagnetically in the optimized, slightly distorted and compositionally rearranged structures. A ferromagnetic coupling is found in the more distorted structures.

INTRODUCTION
Regular full Heusler compounds represent a class of X_2YZ compounds, where X is a transition metal element, Y a transition, rare earth or alkaline earth element and Z a main group element (Graf *et al.*, 2011). They exhibit exceptional properties, key of which is magnetic properties from a combination of non magnetic elements, like in the case of Mn_2VAl (Sanvito *et al.*, 2017). Apart from having a net magnetic moment, many Heusler systems have an electronic structure that is spin polarized at the Fermi level, resulting in half-metallicity, a very useful property in spintronics. Half metallic materials can be used to control the magnetic properties of existing electronics, by the introduction of a spin polarized current into the standard industrial semiconductors such as silicon. They exhibit high tunability, high Curie temperatures and can have extremely diverse compositions (You *et al.*, 2019). Additionally, Heusler 's have the same crystallographic structure as semiconductors and since the discovery of the first half metallic material, NiMnSb in 1983, a sequence of experimental as well as theoretical efforts have been carried out to predict novel semiconductor or half-metallic systems (Khandy *et al.*, 2019)

Heusler compounds are especially experiencing renewed interest due to the realization of materials that are applicable in semiconductor spintronics and magnetoelectronics, such as spin gapless semiconductors in Mn_2 rich Heusler compounds. In spin gapless semiconductors, one spin channel has a zero band gap, while the other has the usual energy gap at the Fermi level. In particular, the conduction and valence band edges of the majority electrons touch at the Fermi energy,

resulting in a zero band gap in the majority channel. In such a material, no threshold energy is required to move electrons from occupied states to empty states. In addition, both holes and electrons can be a hundred percent spin polarized, leading to new functionalities in devices (Ouardi *et al.*, 2013). Spin- filter materials can be made from ferromagnetic or ferrimagnetic semiconducting Heusler compounds and are of particular interest since the mobility of carriers is larger than in usual semiconductors (Galanakis *et al.*, 2014). Spin gapless semiconductors bridge the gap between semiconductors and half-metallic ferromagnets (Chen *et al.*, 2018).

Mn_2CoAl has been demonstrated both from experiment and theoretical investigations to exhibit the spin gapless property (Wei *et al.*, 2018 ; Zhou *et al.*, 2016). It has been reported to be a ferromagnetic spin gapless semiconductor (SGS) with complete spin polarization (Zhou *et al.*, 2015). However, a study of the electronic properties of Mn_2CoAl using the Generalised Gradient Approximation (GGA) to treat the exchange–correlation energy and the Beck-Johnson (mBJ) approach, found it to exhibit a half-metallic (HM) character with 100% spin polarization at the Fermi level. Ferromagnetism with a total magnetic moment of 2 μ_B was found, with the Hg_2CuTi structure being more energetically favourable than the $L2_1$, Cu_2MnAl type structure (Mokhtari *et al.*, 2020).There have however also been reports of bulk Co_2MnAl crystallizing in the $L2_1$ structure, from experimental studies, obtained by induction melting and 10 day annealing at 600–1190 °C under a magnetic field of 5 kOe9 (Zhu and Zhao, 2017). However, Graf, *et al.*, (2009), reports that the Cu_2MnAl and the Hg_2CuTi structures are hardly distinguishable by X- ray diffraction. Care has to be taken in structural analysis, as both have general fcc like symmetry (Graf *et al.*, 2009).

There have been studies on the effect of disorder and lattice distortion on electronic and magnetic properties of Mn_2CoAl. The magnetic moments of Mn were found to be reduced from the predicted value due to structural disorder from a study of the magnetic properties of epitaxially grown thin films of Mn_2CoAl studied using X-ray magnetic circular dichroism, (Jamer *et al.*, 2014). Tetragonalization of the lattice, which can occur during films growth was shown not to have an effect on the spin gapless character of the perfect cubic compound by employing *ab initio* electronic structure calculations on Mn_2CoAl Heusler compound. However atomic swaps were found to destroy the spin gapless character giving rise to a half-metallic state (Galanakis *et al.*, 2014).

In a recent study in which experimental data, and band structure calculations that included disorder were compared, as-prepared Mn_2CoAl film was reported to be best described as a disordered metal, rather than a spin gapless semiconductor (Buckley *et al.*, 2019). In yet another study of a stoichiometric Mn_2CoAl Heusler alloy, the main phase was found to be $Mn_{1.8}Co_{1.4}Al_{0.8}$, rather than Mn_2CoAl. The $Mn_{1.8}Co_{1.4}Al_{0.8}$ phase was found to be a disordered inverse XA Heusler structure with, Mn (A) and Al (C) sites partially substituted by Co and Mn respectively. The disordered structure was found to be half metallic from first-principles calculations although annealed stoichiometric Mn_2CoAl exhibited semiconducting-like resistivity and low anomalous Hall conductivity. An analysis of microstructure seemed to suggest charge localization due to intersection of the Fermi level with Mn 3*d* and Co 3*d* states in $Mn_{1.8}Co_{1.4}Al_{0.8}$ to be the cause for the semiconductor like resistivity, rather than a signature of a spin gapless semiconductor (Xu *et al.*, 2019).

From the foregoing, the importance of the technologically relevant properties of Mn_2CoAl Heusler system is evident. The understanding of these properties, leading to a proper classification and a deeper understanding of the mechanism at the atomic level influencing these properties, will lead to a faster industrial application and exploitation in design of spintronic and magnetoelectronic devices using Mn_2CoAl Heusler compound. In this Density Funtional Theory (DFT) study, as implemented in the Quantum ESPRESSO code, structural optimization of Mn_2CoAl has been carried out, followed by electronic structure calculations for disordered and structurally distorted Heusler system, as a first and preliminary study, of a series of investigations on the Mn_2CoAl Heusler system. The effect on the site resolved atomic magnetic moments for the various systems has been reported.

Computational Details

DFT calculations as implemented in the Quantum ESPRESSO code were performed to determine the structural, electronic and magnetic properties of Mn_2CoAl. The self-consistent Projector Augmented Wave (PAW) approach (Blöchl, 1994) employing the Perdew-Burke-Ernzerhof parametrization of the Generalized Gradient Approximation, (GGA-PBE), to treat the exchange and correlation for the stoichiometric Mn_2CoAl, in the Hg_2CuTi and $L2_1$ full Heusler structure, was employed to carry out a spin polarized investigation. The structural optimizations and electronic structure are conducted using the Broyden–Fletcher–Goldfarb–Shanno (BFGS) minimization. A Monkhorst–Pack uniform K point grid with 4 x 4 x 4 **k** points was chosen for static total energy calculations until a stopping criterion of energy change less than 10^{-4} a.u. was attained. The integration over the irreducible part of the Brillouin zone was done using the Marzari-Vanderbilt smearing method with a Gaussian spreading of 0.05, using uniform cut-off energy for wavefunctions of 80 Ry.

RESULTS AND DISCUSSIONS

In this section, the structural, properties will be discussed. The electronic and magnetic properties for the most stable structure will then be discussed, followed by those of the distorted and disordered structures.

Structural Properties

Structural optimization for X_2YZ Heusler, Mn_2CoAl, in the inverse and $L2_1$ crystal structures, whose prototypes are Hg_2CuTi and Cu_2MnAl respectively, was carried out using the PBE-GGA exchange and correlation approximation. The inverse Heusler structure with space group F43m, space group no. 216, is commonly observed if the atomic number of Y is higher than the one of X from the same period, as is the case for Co and Mn in Mn_2CoAl. The Wyckoff positions for X are 4a (0, 0, 0) and 4d (3/4, 3/4, 3/4), while the Y and the Z atoms are located at 4b (1/2, 1/2, 1/2) and 4c (1/4, 1/4, 1/4), respectively (Graf *et al.*, 2011; Chen *et al.*, 2015; Graf *et al.*, 2009). The $L2_1$ structure belongs to the Fm-3m space group, space group number 225. The Mn atoms occupy the 8c (¼, ¼, ¼) sites, while the Co and Al atoms occupy the 4b (½, ½, ½) and 4a (0, 0, 0) positions respectively. An equivalent $L2_1$ structure would have the X, Y and Z atoms in the 8c (¼, ¼, ¼), 4a (0, 0, 0) and 4b (½, ½, ½) positions respectively (Enamullah *et al.*, 2015). The 1 x 1 x1 unit cells used in this work, having 16 atoms each in the two crystal structures are shown in Fig 1.

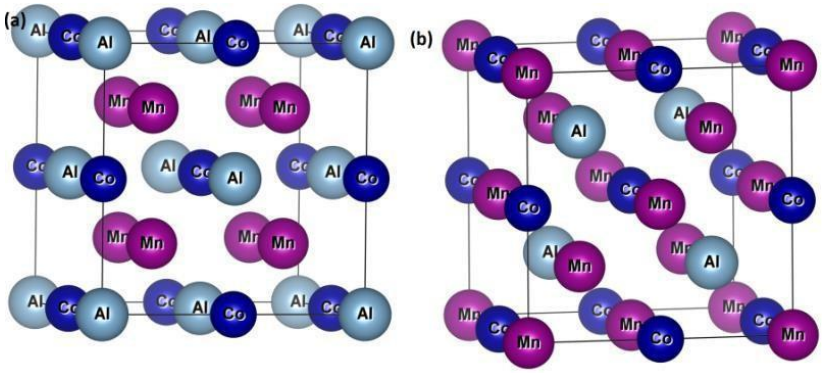

Fig.1 (a): $L2_1$ structures in which Mn occupies the 8 equivalent 8c (¼, ¼, ¼) sites, while

Mn_2CoAl is found to be more stable in the Hg_2CuTi structure than the $L2_1$ structure as shown in Fig.2.

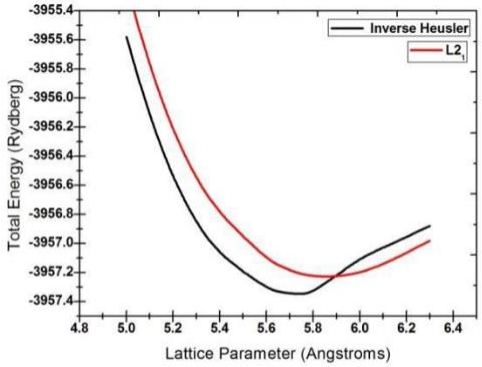

The optimized lattice parameter for the inverse structure is found to be 5.75 Å, while that of the $L2_1$ structure is found to be slightly larger at 5.85 Å. This value compares well with previous studies, in which the lattice parameter for the inverse Heusler structure has been found to be 5.73 Å and 5.787 Å, while employing the GGA approximation (Mokhtari *et al.*, 2020; Chen *et al.*, 2015).

Electronic properties

In this section, the electronic structure for the optimized as well as compositionally and structurally distorted structures

are discussed. The electronic structure for the optimized inverse Heusler system reveals a near zero energy gap feature in the majority states, and a clear energ gap in the minority states. A very small section of the majority valence states intersect the Fermi level as shown in Fig. 3. A closer look at the orbital contribution of the *d* wave functions at the Fermi level reveals that the *d* states of one of the Mn (2) atoms have slightly higher energies, resulting in their intersection of the Fermi level, as well as a much smaller contribution from the *d* states of the Co and Mn (1) atom.

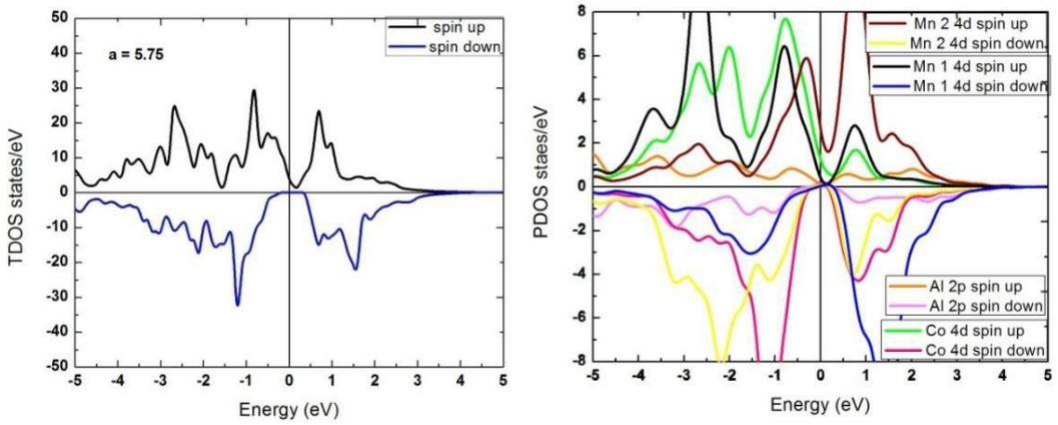

Fig. 3: Total Density of States (TDOS) and Projected Density of States (PDOS) for optimized inverse Heusler structure of Mn_2CoAl

An introduction of a small tetragonal distortion of the inverse cubic unit cell, such that the c/a ratios are 0.97 and 1.03, resulted in slightly more states intersecting the Fermi level, with increasing distortion, thereby, tending more towards a half metallic electronic structure rather than a spin gapless electronic structure as shown in Fig. 4.

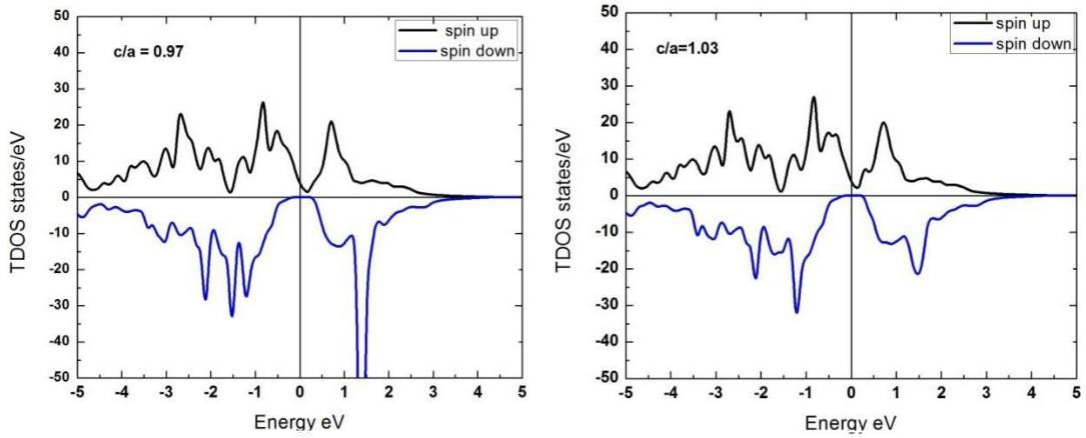

For higher distortions such that the c/a ratios are 0.688 and 1.52, the metallic character emerges as shown in Fig. 5 and 6, with sharp peaks appearing at the Fermi level, which is indicative of structural instability.

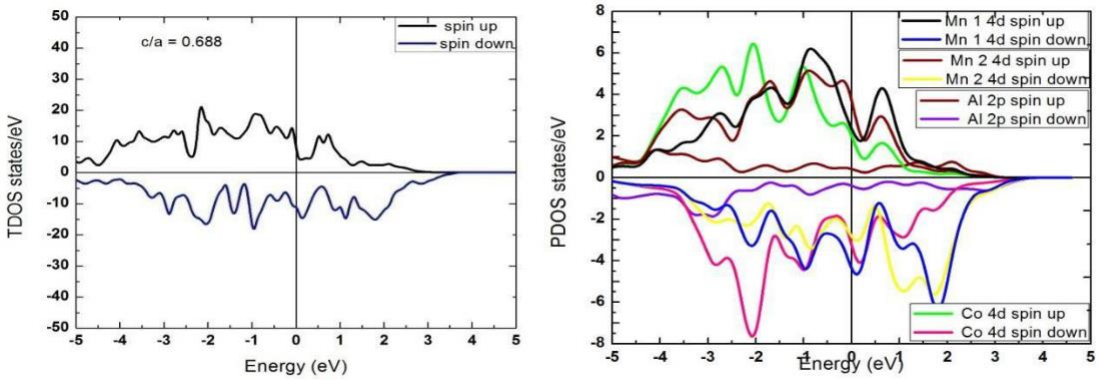

Fig. 5: Total Density of States (TDOS) and Projected Density of States (PDOS) for Mn_2CoAl with c/a ratio of 0.688.

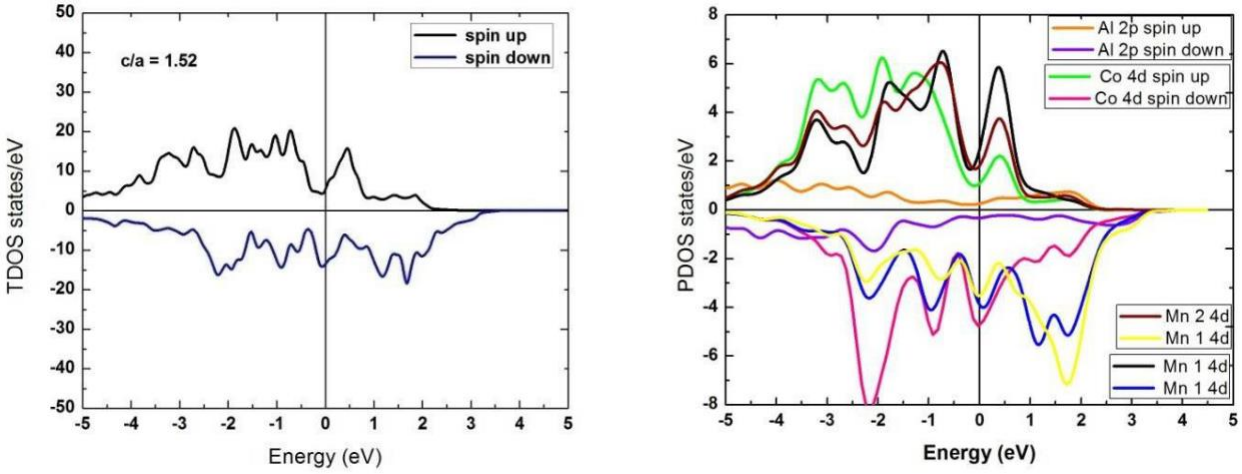

Fig. 6: Total Density of States (TDOS) and Projected Density of States (PDOS) for Mn_2CoAl with c/a ratio of 1.52

The electronic structure for the $L2_1$ structure was also studied, even though it was found to have higher energy, so as to better understand the interaction between the *d* states when the Mn atoms occupy equivalent positions. In Fig 7, it is evident that the Mn states have the same energy for both atoms. Their hybridization causes their states to be pushed to lower energies, hence reducing the majority states at the Fermi level.

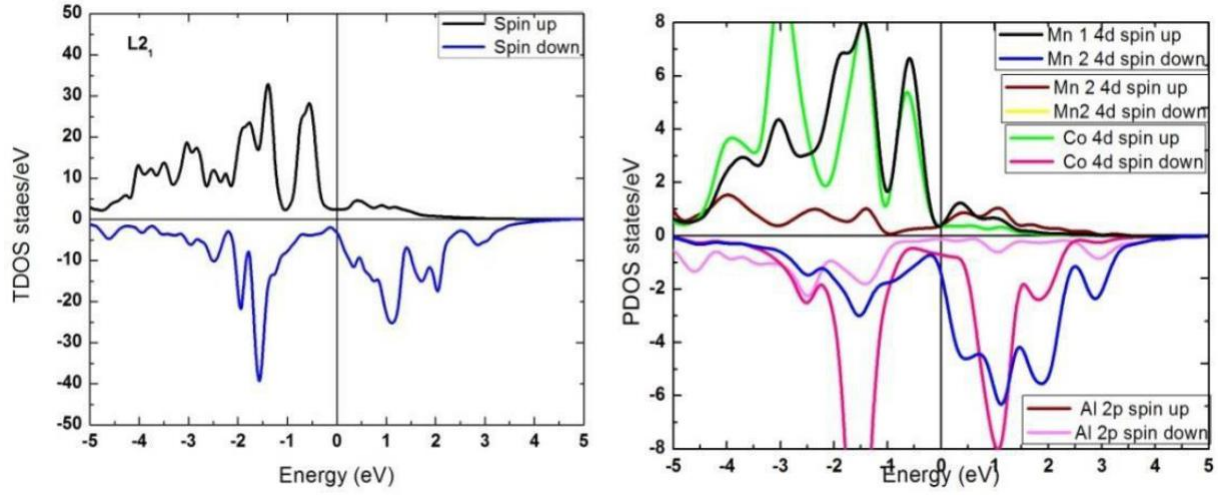

Fig. 7: Total Density of States (TDOS) and Projected Density of States (PDOS) for optimized $L2_1$ structure of Mn_2CoAl

However, the semiconducting gap in the minority states is destroyed, with the Co *d* states being pushed to lower energies. The electronic structure is metallic, with both spin channels conducting and a ferromagnetic coupling between all the transition metal elements.

The effect of mixing the Co and Mn sites in the inverse structure resulted in a half metallic electronic structure as shown in Fig 8, arising from hybridization of *d* states of the transition metal elements.

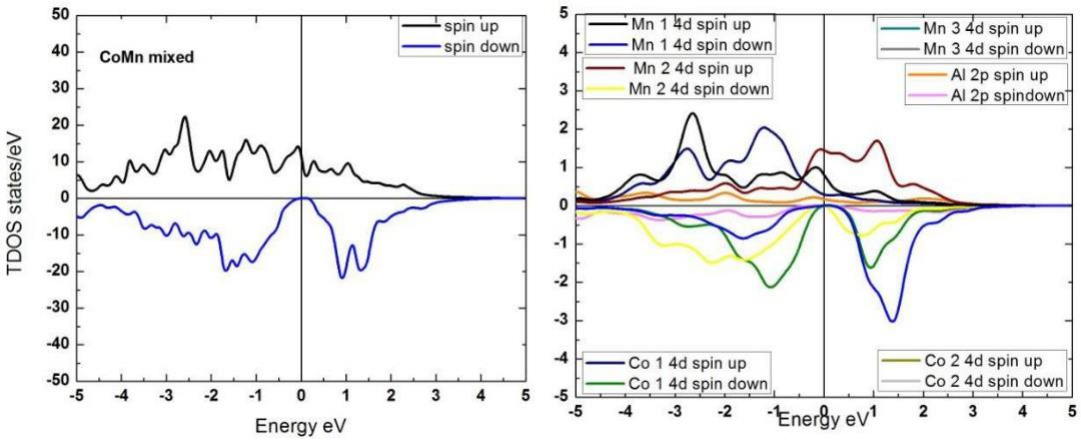

Fig. 8: Total Density of States (TDOS) and Projected Density of States (PDOS) for

Magnetic properties

In this section, the atom resolved magnetic moments for the various systems are discussed. Table one summarizes the site resolved magnetic moments for the atoms.

Table 1: Site resolved magnetic moments for the Mn_2CoAl atoms

c/a ratio	Magnetic Moments (μB)			
	Mn(1)	Mn(2)	Co	Al
c/a =1	-1.848	2.659	0.729	-0.025
c/a = 0.970	-1.853	2.659	0.728	-0.024
c/a = 1.030	-1.852	2.658	0.726	-0.024
c/a = 0.688	1.212	1.624	0.841	-0.025
c/a = 1.520	1.449	2.064	0.980	-0.053
Co Mn mixed	-1.784	2.429	1.050	-0.028

The two Mn atoms couple ferrimagnetically for the optimized structure and for the slightly distorted structures, as well as the compositionally rearranged structure. However, in the more distorted structures, they couple ferromagnetically. Mokhtari *et al*., (2020), found a magnetic moment of 2.550 μB on the Mn(2) atom, using the GGA approximation, which compares well with the value of 2.659 μB found in this study. In other works, the value was found to be 2.800 μB, which also coupled ferrimagnetically with the second Mn atom (Mokhtari *et al.*, 2020; Galanakis *et al.*, 2014)). Intermixing the Co and Mn sites leads to a reduction of the magnetic moment of Mn (2) atom to 2.429 μB, evidently due to the increased hybridization between the Mn (2) and Co *d* states due to better overlap of the orbitals as shown in Fig. 8. Contracting the structure causes the magnetic moment for the Mn (2) atom to decrease, while expanding causes it to increase. For a lattice constant of 5.65 Å, 5.70 Å and 5.80 Å, the magnetic moments are 2.416 μB, 2.539 μB and 2.769 μB respectively. This is as a result of increased hybridization in the contracted structure due to enhanced overlap of the orbitals upon contraction.

CONCLUSION

In this study, Mn_2CoAl has been found to be more stable in the inverse Heusler structure. The electronic structure reveals almost vanishing states at the Fermi level in the majority states, explaining why Mn_2CoAl has been classified as half metallic rather than spin gapless in some studies. We find Mn *d* states intersecting the Fermi level to a slightly greater extent than the Co *d* states, which altogether are however very few. The electronic structure from this study therefore is half metallic rather than spin gapless. The Mn magnetic moments are ferrimagnetically coupled in the optimized inverse structure and reduce as a result of compositional rearrangement of the atoms. Upon structural distortion, the magnetic moments remain constant except for greater distortions of the structure. Further treatment of the *d* states of the transition metal elements, taking into account their localization in the next part of this series, will provide a more definite description of the electronic structure of this interesting system

ACKNOWLEDGEMENTS
The author acknowledges the Centre for High Performance Computing (CHPC), South Africa, for providing computational resources to this research project.

REFERENCES

Blöchl, P. E. (1994). Projector augmented-wave method. *Phys. Rev. B* **50**, 17953–17979.

Buckley, R. G., Butler, T., Pot, C., Strickland, N. M., and Granville, S. (2019). Exploring disorder in the spin gapless semiconductor Mn_2CoAl. *Mater. Res. Express* **6**, 106113.

Chen, P., Gao, C., Chen, G., Mi, K., Liu, M., Zhang, P., and Xue, D. (2018). The low-temperature transport properties of Heusler alloy Mn_2CoAl. *Appl. Phys. Lett.* **113**, 122402.

Chen, X.-R., Zhong, M.-M., Feng, Y., Zhou, Y., Yuan, H.-K., and Chen, H. (2015). Structural, electronic, elastic, and thermodynamic properties of the spin-gapless semiconducting Mn_2CoAl inverse Heusler alloy under pressure. *Phys. Status Solidi B* **252**, 2830–2839.

Enamullah, Venkateswara, Y., Gupta, S., Varma, M. R., Singh, P., Suresh, K. G., and Alam, A. (2015). Electronic structure, magnetism, and antisite disorder in CoFeCrGe and CoMnCrAl quaternary Heusler alloys. *Phys Rev B* **92**, 224413.

Galanakis, I., Özdoğan, K., Şaşıoğlu, E., and Blügel, S. (2014). Conditions for spin-gapless semiconducting behavior in Mn_2CoAl inverse Heusler compound. *J. Appl. Phys.* **115**, 93908.

Graf, T., Casper, F., Winterlik, J., Balke, B., Fecher, G. H., and et al (2009). Crystal Structure of New Heusler Compounds. *Journal of Inorganic and General Chemistry* **2009**, 976.

Graf, T., Felser, C., and Parkin, S. S. P. (2011). Simple rules for the understanding of Heusler compounds. *Prog. Solid State Chem.* **39**, 1–50.

Jamer, M. E., Assaf, B. A., Sterbinsky, G. E., Upton, NY, Arena, D. A., and Heiman, D. [Northeastern U., Boston, MA . (2014). Atomic moments in Mn_2CoAl thin films analyzed by X-ray magnetic circular dichroism. *J. Appl. Phys.*

Khandy, S., Islam, I., Gupta, D., Khenata, R., and Laref, A. (2019). Lattice dynamics, mechanical stability and electronic structure of Fe-based Heusler semiconductors. *Scientific Reports* **9**.

Mokhtari, D. J., Jum'h, I., Baaziz, H., Charifi, Z., Ghellab, T., Telfah, A., and Hergenröder, R. (2020). Structural, electronic, magnetic and thermoelectric properties of inverse Heusler alloys Ti_2CoSi, Mn_2CoAl and Cr_2ZnSi by employing Ab initio calculations. *Philos. Mag.* **100**, 1636–1661.

Ouardi, S., Fecher, G. H., Felser, C., and Kübler, J. (2013). Realization of spin gapless semiconductors: the Heusler compound Mn_2CoAl. *Phys. Rev. Lett.* **110**, 100401.

Sanvito, S., Oses, C., Xue, J., Tiwari, A., Zic, M., Archer, T., Tozman, P., Venkatesan, M., Coey, M., and Curtarolo, S. (2017). Accelerated discovery of new magnets in the Heusler alloy family. *Sci. Adv.* **3**, e1602241–e1602241.

Wei, M.-S., Cui, Z., Ruan, X., Zhou, Q.-W., Fu, X.-Y., Liu, Z.-Y., Ma, Q.-Y., and Feng, Y. (2018). Interface Characterization of Current-Perpendicular-to-Plane Spin Valves Based on Spin Gapless Semiconductor Mn2CoAl. *Appl. Sci.* **2018**.

Xu, X. D., Chen, Z. X., Sakuraba, Y., Perumal, A., Masuda, K., Kumara, L. S. R., Tajiri, H., Nakatani, T., Wang, J., Zhou, W., Miura, Y., Ohkubo, T., and Hono, K. (2019). Microstructure, magnetic and transport properties of a Mn2CoAl Heusler compound. *Acta Mater.* **176**, 33–42.

You, J., Cao, J., Khenata, R., Wang, X., Shen, X., and Yang, T. (2019). Robust Spin-Gapless Behavior in the Newly Discovered Half Heusler Compound MnPK. *Mater. Basel Switz.* **12**.

Zhou, H., Liu, X., Yang, B., Qu, Y., Bu, H., and Zhao, M. (2016). Electron spin-polarization and spin-gapless states in an oxidized carbon nitride monolayer. *RSC Adv* **6**, 108280–108285.

Zhou, J., Sa, B., Sun, Z., Si, C., and Ahuja, R. (2015). Manipulating carriers' spin polarization in the Heusler alloy Mn_2CoAl. *RSC Adv* **5**, 73814–73819.

Zhu, L. J. and Zhao, J. H. (2017). Anomalous resistivity upturn in epitaxial $L2_1$-Co_2MnAl films. *Sci. Rep.* **7**, 42931.

****